Theoretical Population Biology **59**, 157–174 (2001)
doi:10.1006/tpbi.2000.1509, available online at http://www.idealibrary.com on IDEAL®

Wave of Chaos: New Mechanism of Pattern Formation in Spatio-temporal Population Dynamics

Sergei V. Petrovskii

Shirshov Institute of Oceanology, Russian Academy of Sciences, Nakhimovsky Prospect 36, Moscow 117218, Russia
E-mail: spetrovs@sio.rssi.ru

and

Horst Malchow

Institute of Environmental Systems Research, Department of Mathematics and Computer Science, University of Osnabrück, Artilleriestrasse 34, D-49069 Osnabrück, Germany
E-mail: malchow@uos.de

Received November 9, 2000

The dynamics of a simple prey–predator system is described by a system of two reaction-diffusion equations with biologically reasonable non-linearities (logistic growth of the prey, Holling type II functional response of the predator). We show that, when the local kinetics of the system is oscillatory, for a wide class of initial conditions the evolution of the system leads to the formation of a non-stationary irregular pattern corresponding to spatio-temporal chaos. The chaotic pattern first appears inside a sub-domain of the system. This sub-domain then steadily grows with time and, finally, the chaotic pattern invades the whole space, displacing the regular pattern.

1. INTRODUCTION

The issue of spatial and spatio-temporal pattern formation in biological communities is probably one of the most exciting problems in modern biology and ecology. It is one of the typical features of the dynamics of both aquatic and terrestrial populations in their natural environment. Sometimes, the reasons for the spatial heterogeneity of the species distribution are more or less obvious. Thus, the consideration of the functioning of a biological community in a fragmented habitat leads to the concept of spatially structured populations (Levin *et al*., 1993; Hanski and Gilpin, 1997; Hanski, 1999). Another explanation of animal grouping can be found in the social behaviour of higher-organized species like flocks of birds, schools of fish, etc. (Okubo, 1986; Flierl *et al*., 1999). However, there are a number of examples where animal aggregation cannot immediately be attributed to an apparent reason.

For instance, it is well known that the spatial horizontal distribution of plankton in the natural marine environment is highly inhomogeneous (Fasham, 1978; Mackas and Boyd, 1979; Greene *et al*., 1992). The data of observations show that, on a spatial scale of dozens of kilometers and more, the plankton patchy spatial distribution is mainly controlled by the inhomogeneity of underlying hydrophysical fields like temperature and nutrients (Denman, 1976; Weber *et al*., 1986). On a scale of less than one hundred meters, plankton patchiness is controlled by turbulence (Platt, 1972; Powell *et al*.,

0040-5809/01 $35.00

1975). However, the features of the plankton heterogeneous spatial distribution are essentially different (uncorrelated with the environment) on an intermediate scale, roughly, from a hundred meters to a dozen kilometers (Powell *et al*., 1975; Weber *et al*., 1986); also see (Seuront *et al*., 1999). This distinction is usually considered evidence of the biology's "prevailing" against hydrodynamics on this scale (Levin, 1990; Powell, 1995).

This problem generated a number of hypotheses about the possible origin of the spatially heterogeneous distribution of species in nature. Several possible scenarios of pattern formation were proposed; cf. Malchow (2000a) for a brief summary. Using non-linear partial differential "diffusion-reaction" equations as a mathematical tool (Vinogradov and Menshutkin, 1977; Okubo, 1980; Murray, 1989; Shigesada and Kawasaki, 1997), many authors attribute the formation of spatial patterns in natural populations to well-known general mechanisms, e.g., to differential-diffusive Turing (Turing, 1952; Segel and Jackson, 1972) or differential-flow-induced (Rovinsky and Menzinger, 1992) instabilities; cf. Malchow (1996, 2000b). However, these theoretical results, whatever their importance in a general theoretical context, are not directly applicable to the problem of spatial pattern formation in plankton. Actually, the formation of "dissipative" Turing patterns is only possible under the limitation that the diffusivities of the interacting species are not equal. This is usually not the case in a planktonic system where the dispersal of species is due to turbulent mixing. Also (and this is probably more important) the patterns appearing as a result of a Turing instability are typically stationary and regular while the spatial distribution of plankton species in a real marine community is non-stationary and irregular. The impact of a differential or shear flow may be important for pattern formation in a benthic community as a result of tidal forward–backward water motion (Malchow and Shigesada, 1994) but seems to be rather artificial concerning the pelagic plankton system. Again, the patterns appearing according to this scenario are usually highly regular which is not realistic.

Although the importance of ecological interactions for the formation of spatial patterns is widely recognized (Levin *et al*., 1993; Powell, 1995), the effect of particular processes can be different in different circumstances. A number of authors propose problem-oriented approaches relating pattern formation to a specific inhomogeneity of certain ecosystem parameters (Pascual, 1993), to particular hydrodynamical processes (Dubois, 1975; Pedley and Kessler, 1992; Malchow and Shigesada, 1994; Abraham, 1998), or to the special choice of initial conditions (Sherratt *et al*., 1995). It seems, however, that these important theoretical results do not provide a complete, satisfactory solution of the problem. Since spatio-temporal pattern formation in natural biological communities is so common, one can expect that besides the mechanisms listed above which are apparently responsible for inhomogeneous species distributions in many particular situations, there might exist a more general mechanism, not necessarily depending on particular or specific conditions.

This reflection can serve as the starting point for choosing an adequate mathematical model. Such a model, which should display certain "intrinsic" mechanisms of pattern formation, must only account for features which are common for various biological communities. The choice of the "most common" biological properties seems to be rather disputable. Here, we take the view that it is the trophical connection that is both common and strong, actually integrating different species into a community (Vinogradov, 1983).

With these suppositions, one can conclude that the formation of spatio-temporal patterns in a biological community is, in some sense, a direct consequence of the interspecific interactions. One way to verify these ideas is to consider the dynamics of a distributed two-species prey–predator model (another approach could be a host–parasitoid model; cf. Comins *et al*. (1992)). If the hypotheses are true, such a model, with biologically reasonable functional responses, should be capable of describing the formation of realistic irregular spatio-temporal patterns.

A widespread opinion, however, still is that a two-component diffusion-reaction system is too simple to provide a realistic "image" of real processes. Examples of complex spatio-temporal behaviour of two-species systems with oscillatory local kinetics (e.g., Kopell and Howard, 1973; Murray, 1989; Ermentrout *et al*., 1997) are usually associated with the specific choice of finite initial conditions (Sherratt *et al*., 1995; Merkin *et al*., 1996; Davidson, 1998). In fact, this restriction is not necessary. Recently, a non-Turing mechanism of pattern formation free from the usual constraints has been reported by Petrovskii and Malchow (1999). The formation of irregular spatio-temporal patterns in a prey–predator model with spatially uniform system parameters appears for a wide class of initial conditions; in that sense a complex dynamics is typical for two-species systems.

In this paper we present the results of a detailed investigation of a simple prey–predator mechanism. The mathematical model is formulated in Section 2. Furthermore, the local dynamics of the system is considered. Section 3 gives the results of numerical experiments for various initial conditions and provides an *in situ* description of the phenomenon. Section 4 contains the results of

the analytical calculation of the speed of the interface separating the sub-domains occupied by different patterns. Section 5 deals with the persistence of different patterns and characteristic time scales. The spatial correlation of species variations is considered in Section 6. The paper closes with the discussion of the results in Section 7.

2. MAIN EQUATIONS

We consider the spatio-temporal dynamics of a relatively simple two-species prey–predator community which can be described by the following one-dimensional reaction-diffusion equations (Segel and Jackson, 1972; Levin *et al.*, 1993; Murray, 1989; Shigesada and Kawasaki, 1997):

$$u_t = Du_{xx} + f(u, v), \tag{1}$$

$$v_t = Dv_{xx} + g(u, v). \tag{2}$$

Here, $u(x, t)$ and $v(x, t)$ are the concentrations of prey and predator, respectively, x is the spatial coordinate, t is the time, and D is the diffusion coefficient. Since we are especially interested in the possibility of non-Turing pattern formation, we assume that the diffusivities are equal for both species. This is the usual case for natural plankton communities where the mixing is mainly caused by marine turbulence. The form of the functions $f(u, v)$ and $g(u, v)$ is determined by the local biological processes in the community. For biological reasons, they must have the following structure: $f(u, v) = P(u) - E(u, v)$ and $g(u, v) = \kappa E(u, v) - \mu v$. The function $P(u)$ describes the local growth and natural mortality of the prey whereas $E(u, v)$ describes the trophical interaction of the species, i.e., predation. The term μ is the mortality rate of the predator and κ the coefficient of food utilization.

The particular choice of the functions $P(u)$ and $E(u, v)$ in Eqs. (1) and (2) may be different, depending on the type of prey population and on the type of functional response of the predator. In this paper we assume that the local growth of the prey is logistic and the predator shows type II trophical response. Then, choosing the simplest mathematical expression for $E(u, v)$ (cf. Murray, 1989; Shigesada and Kawasaki, 1997), we arrive at the system

$$u_t = Du_{xx} + \alpha u\left(1 - \frac{u}{b}\right) - \gamma \frac{u}{u+h} v, \tag{3}$$

$$v_t = Dv_{xx} + \kappa\gamma \frac{u}{u+h} v - \mu v. \tag{4}$$

α, b, h, and γ are certain constants: α stands for the maximum *per capita* growth rate of the prey, b is the carrying capacity for the prey population, and h is the half-saturation density of the prey.

The next step is to introduce dimensionless variables. Considering $\tilde{u} = u/b$, $\tilde{v} = v\gamma/(\alpha b)$, $\tilde{t} = \alpha t$, $\tilde{x} = x(\alpha/D)^{1/2}$, from (3) and (4) we obtain

$$\tilde{u}_t = \tilde{u}_{xx} + \tilde{u}(1 - \tilde{u}) - \frac{\tilde{u}}{\tilde{u} + H} \tilde{v}, \tag{5}$$

$$\tilde{v} = \tilde{v}_{xx} + k \frac{\tilde{u}}{\tilde{u} + H} \tilde{v} - m\tilde{v}, \tag{6}$$

where $H = h/b$, $m = \mu/\alpha$, and $k = \kappa\gamma/\alpha$. Thus, one can expect that certain properties of the system behaviour, e.g., the structure of the system's local phase space, may depend only on three dimensionless parameters H, m, and k.

Before proceeding to the study of spatio-temporal pattern formation, the local system dynamics is considered. For notation simplicity, tildes will be omitted now. One finds by linear stability analysis that the system

$$\frac{du}{dt} = u(1 - u) - \frac{u}{u + H} v, \qquad \frac{dv}{dt} = k \frac{u}{u + H} v - mv \tag{7}$$

possesses three stationary states, (0, 0) (total extinction), (1, 0) (extinction of the predator) and the non-trivial state (u_*, v_*) (co-existence of prey and predator), where

$$u_* = \frac{rH}{1 - r} \qquad \text{and} \qquad v_* = (1 - u_*)(H + u_*) \tag{8}$$

with $r = m/k$. It is readily seen that (0, 0) is a saddle point for all non-negative values of k, m, and H. The stationary state (1, 0) is either a saddle point if the co-existence state (u_*, v_*) lies in the biologically reasonable positive quadrant $u > 0$, $v > 0$ or a stable node otherwise. The stationary co-existence (u_*, v_*) can be of any type.

Although the parameter space of Eq. (7) is three-dimensional, the properties of the local dynamics depend mainly on H and the ratio $r = m/k$, showing only a slight explicit dependence on k separately; cf. Petrovskii and Malchow (1999, 2000) for more details. This allows one to present the results of the investigation of the system's local kinetics as a map in the parameter plane (r, H); cf. Fig. 1. Here, domain A1 above curve 1 corresponds to the case of (u_*, v_*) being a saddle point (the only attractor in phase plane (u, v) for these parameter values is the stable node (1, 0)), domain A2 between curves 1 and 3 to (u_*, v_*) being a stable node, and domain A3 between

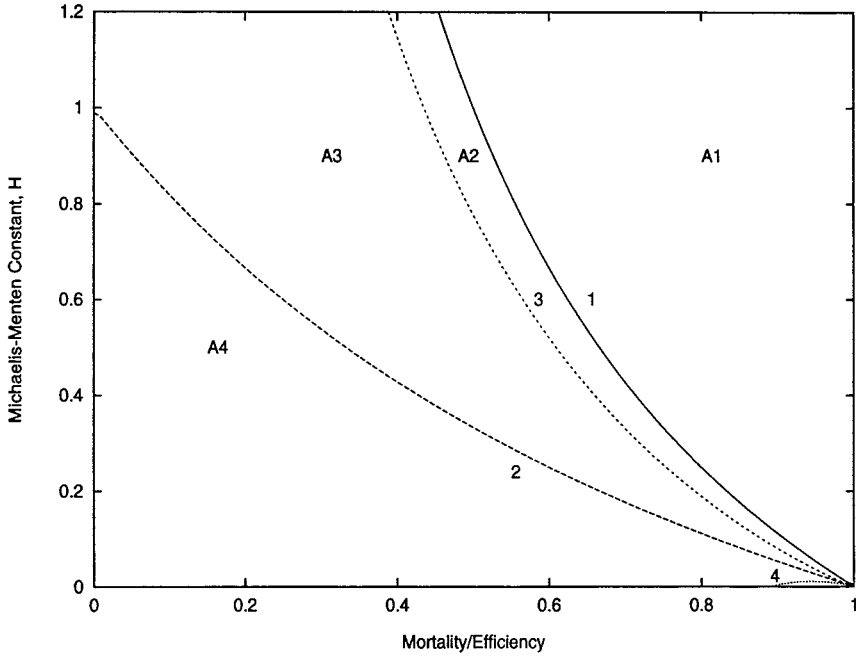

FIG. 1. Map in parameter plane (r, H) for $k = 2.0$; cf. comments in text. The boundaries of the domains are found analytically.

curves 2 and 3 to (u_*, v_*) being a stable focus. Domain A4 between curves 2 and 4 and the domain under curve 4 (cf. the right bottom corner of Fig. 1) correspond to an unstable focus and node, respectively, surrounded by a stable limit cycle which appears via Hopf bifurcation when crossing curve 2. Here, curves 1 and 2 are "universal," i.e., their positions do not depend on k, and curves 3 and 4 show only a slight dependence on k (for values $k \ll 1$ curves 3 and 4 approach curve 2, and for values $k \gg 1$ curve 3 gets close to curve 1 while curve 4 approaches axis r). Note that the oscillatory kinetics of the system becomes somewhat different when the point in the parameter plane (r, H) is moving farther away from curve 2: the limit cycle grows in size and approaches the axes u and v, and the period of the limit cycle grows significantly whereas the motion along the cycle becomes strongly non-uniform.

These results provide helpful information as to which parameter values should be chosen for numerical simulations of the full problem (5)–(6). If the stable stationary "co-existence" state in phase space (domains A2 and A3) exists, the dynamics of the system is typically reduced to the relaxation to the stable stationary spatially homogeneous state $u(x, t) \equiv u_*$, $v(x, t) \equiv v_*$. The details of the process depend on the type of the initial conditions, e.g., for a finite initial distribution of species the relaxation usually takes place after propagation of diffusive fronts (Dunbar, 1986; Murray, 1989; Petrovskii *et al.*, 1998; Petrovskii and Malchow, 2000). Since in this paper we are more concerned with the formation of non-stationary spatio-temporal patterns, parameter values from the domains below curve 2 are of primary interest (Sherratt *et al.*, 1995; Petrovskii and Malchow, 1999).

3. RESULTS OF COMPUTER SIMULATIONS: ORDER DISPLACED BY CHAOS

To investigate the spatio-temporal dynamics of the system, Eqs. (5) and (6) are solved numerically by a finite-difference method. We use a semi-implicit two-layer scheme. At each time step, the diffusion terms are approximated with finite differences on the upper layer and the reaction terms are taken from the lower layer. The mesh step sizes Δx and Δt are chosen sufficiently small so that the results do not show any visible dependence on the step size. Furthermore, considering various forms of the non-linearities in Eqs. (5) and (6), we tested the method by comparing the numerical results with some known analytical predictions (Dunbar, 1986; Murray, 1989, p. 279).

The spatio-temporal dynamics of the system depends to a large extent on the choice of initial conditions. Recently, Eqs. (5) and (6) have been considered in a few

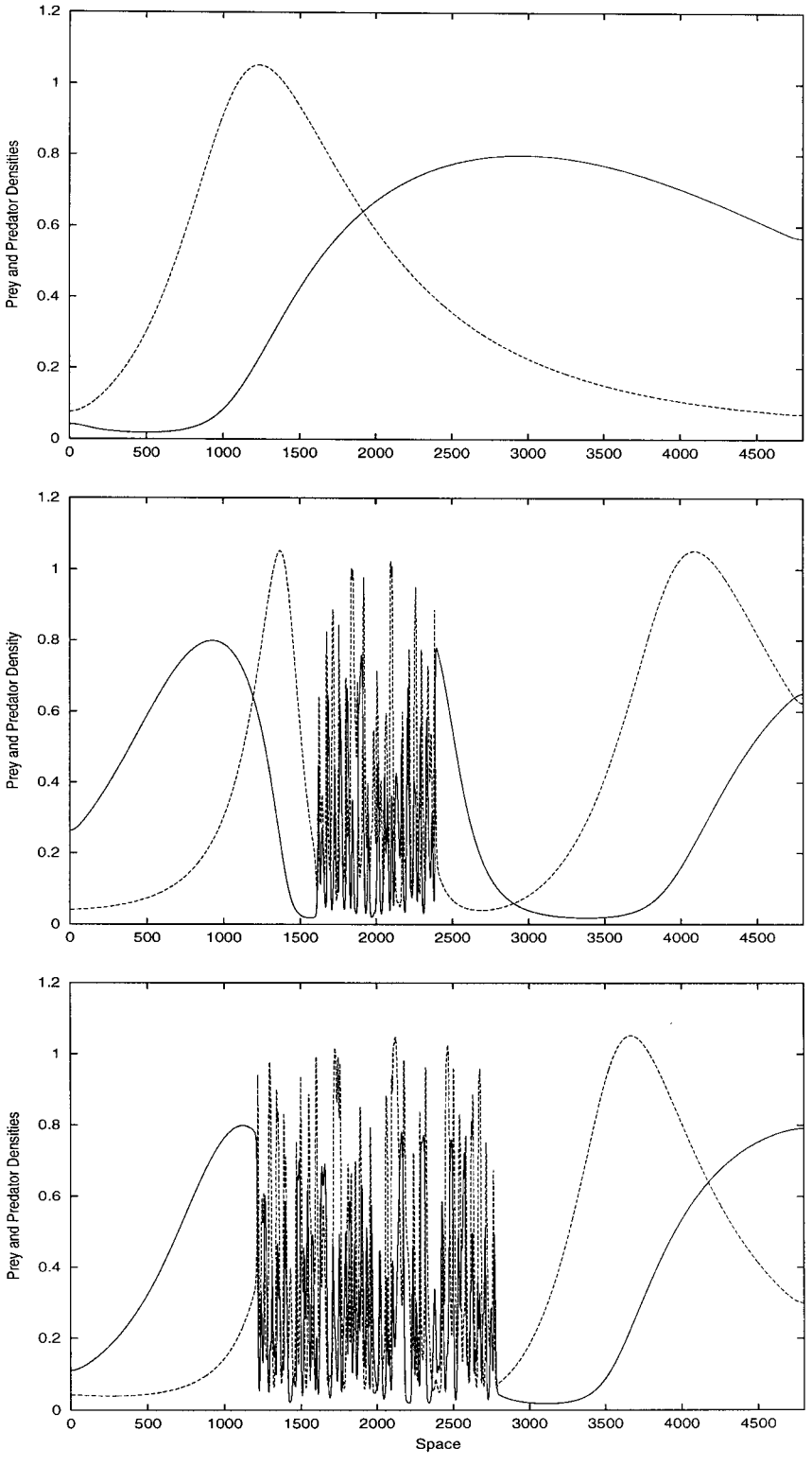

FIG. 2. Typical spatial distribution of species (solid line for prey, dashed for predator) obtained from initial conditions (9) and (10) in the case of "smooth" (regular) pattern formation (top, at $t = 1600$ for parameters $k = 2.0$, $r = 0.4$, $H = 0.3$, $\varepsilon = 10^{-5}$, and $\delta = 10^{-2}$) and "sharp" (chaotic) pattern formation (middle and bottom, at $t = 1000$ and $t = 2000$, respectively, obtained for $\varepsilon = 2 \times 10^{-5}$ and $\delta = -4 \times 10^{-2}$; other parameters are the same).

papers (Sherratt *et al.*, 1995; Shigesada and Kawasaki, 1997; Petrovskii *et al.*, 1998; Petrovskii and Malchow, 2000) in connection with the problem of biological invasion when the initial conditions are usually described by finite functions and the dynamics of the community consists mainly of a variety of diffusive populational fronts. In this paper we are interested in another situation. Namely, we suggest that, at the beginning of the process, both populations are spread over the whole area. In a real community, the details of the initial spatial distribution of the species can be caused by quite specific reasons. The simplest and, in some sense, most general form of the allocated initial distribution would be spatially homogeneous initial conditions. However, in this case the distribution of the species stays homogeneous forever and no spatial pattern can emerge. In order to induce a non-trivial spatio-temporal dynamics, one has to perturb the homogeneous distribution. In this paper, a few different forms of the "disturbed" initial conditions will be considered. We begin with the constant-gradient distribution,

$$u(x, 0) = u_*, \tag{9}$$

$$v(x, 0) = v_* + \varepsilon x + \delta, \tag{10}$$

where ε and δ are certain parameters. The type of system dynamics is determined by the values of ε and δ. When ε is small, the initial conditions (9) and (10) evolve to a smooth non-monotonic spatial distribution of species. Figure 2 (top) shows concentrations u and v at $t = 1600$ obtained for parameters $k = 2.0$, $r = 0.4$, $H = 0.3$, $\varepsilon = 10^{-5}$, and $\delta = 10^{-2}$. The spatial distributions gradually vary in time, and the local temporal behaviour of the dynamical variables u and v follows the limit cycle of the homogeneous system (Petrovskii and Malchow, 1999).

However, for a slightly different set of parameters (e.g., if the value of the gradient exceeds a certain critical value, $\varepsilon \geqslant \varepsilon_{cr}$, where ε_{cr} may depend on δ), the dynamics of the system undergoes principal changes; see Fig. 2, middle ($t = 1000$) and bottom ($t = 2000$) (calculated for $\varepsilon = 2 \times 10^{-5}$ and $\delta = -4 \times 10^{-2}$; other parameters are as above). In this case, the initial distribution (9)–(10) leads to the formation of a strongly irregular "sharp" non-stationary pattern inside a sub-domain of the system (see Fig. 2, middle). The size of the region occupied by this pattern steadily grows with time (cf. middle and bottom of Fig. 2) and finally irregular spatio-temporal oscillations prevail over the whole domain. The temporal behaviour of the concentrations u and v also becomes completely different. Figure 3 shows the "local" phase

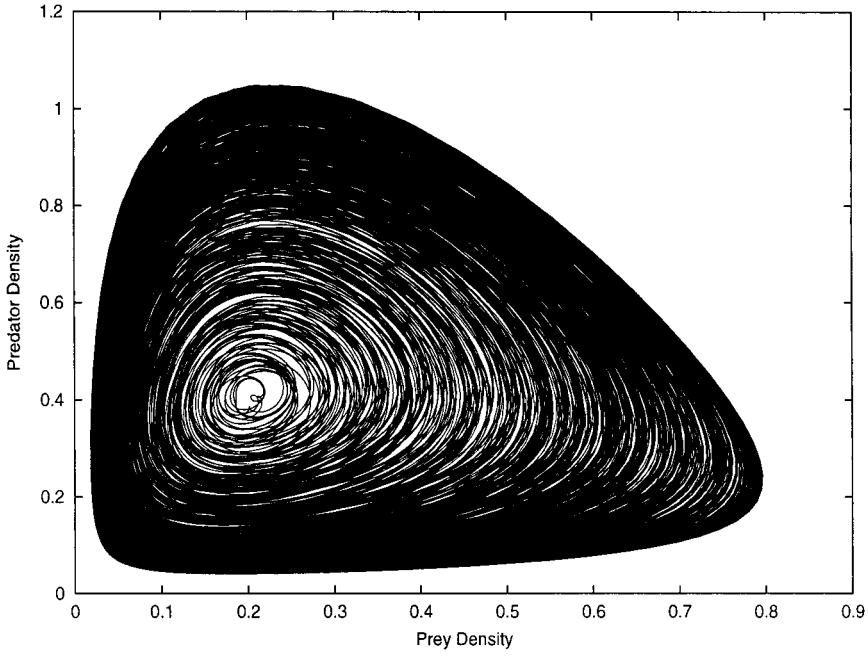

FIG. 3. Local phase plane of the system (5)–(6) after formation of a "sharp" (chaotic) pattern. Parameters are the same as those in Fig. 2 (middle and bottom). The boundary of the domain coincides with the limit cycle.

plane of the system at a fixed point $\bar{x}$ inside the region invaded by the irregular spatio-temporal oscillations. The trajectory fills nearly the whole domain inside the limit cycle.

The apparent irregularity of the system dynamics in the case of the formation of the "sharp" pattern, cf. Figs. 2 (middle and bottom) and 3, gives rise to the question about the degree of this irregularity, particularly, whether this regime of the system dynamics can be classified as chaos. Along with irregularity, chaos means sensitivity to the initial conditions; i.e., the difference between perturbed and unperturbed solutions grows exponentially with time until it is of the same order as the solutions themselves. This feature was proved to be equivalent to some other properties, e.g., to the exponential decay of the autocorrelation function and to a special "flat" form of the power spectrum (cf. Nayfeh and Balachandran, 1995). Furthermore, it can be quantified in terms of the (positive) dominant Lyapunov exponent. Thus, in practice a variety of methods can be applied to reveal chaos. The power spectra of he prey and predator density in model (5)–(6) were analyzed in Petrovskii and Malchow (1999); it was shown that the formation of such irregular spatio-temporal patterns shown in Figs. 2 and 3 corresponds to a chaotic dynamics. The strong sensitivity of the solutions of system (5)–(6) to a small variation of the initial conditions in the parameter range corresponding to the formation of irregular non-stationary patterns is shown in Medvinsky *et al.* (2000); the corresponding value of the dominant Lyapunov exponent is estimated as $\lambda_D \cong 0.001 > 0$. Further on, accounting for these results, we will refer to the "smooth" and "sharp" patterns as regular and chaotic ones.

A remarkable property of the system dynamics is that for each moment of time, there exist distinct boundaries or interfaces, separating the regions of chaotic and regular patterns (cf. Fig. 2, middle and bottom). Our numerical results show that these interfaces propagate with an approximately constant speed in opposite directions, so that the size of the region with chaotic dynamics is always growing until it occupies the whole domain. The width of the front stays approximately constant. Thus, chaos arises as a result of the propagation of the "wave of chaos," i.e., the moving interface between the two regions. The phenomenon is essentially spatio-temporal: the chaos prevails over the regular pattern by "displacing" it.

The dynamics with somewhat more general initial conditions can be even more complicated, showing a phenomenon which may be called "intermittency:" regular and chaotic patterns alternate in space. As a particular example, we consider the following form of the initial conditions:

$$u(x, 0) = u_*, \tag{11}$$

$$v(x, 0) = v_* + \varepsilon x + \delta + \varepsilon_1 \cos\left(\frac{2\pi x}{L}\right). \tag{12}$$

In this case, only slightly disturbed initial conditions (see Fig. 4, top, for $\varepsilon_1 = 0.07$, $\varepsilon = 1.5 \times 10^{-5}$, $\delta = -3.6 \times 10^{-2}$, length $L = 4800$; other parameters are the same as in Fig. 2) evolve to a spatial distribution of species where two regions with chaotic dynamics are separated by regions with regular dynamics; cf. bottom of Fig. 4 at $t = 800$. As in the previous case, the size of the chaotic regions steadily grows so that, finally, the chaotic pattern invades the whole domain.

Since this scenario of pattern formation appears to be essentially different from those already known for two-component diffusion-reaction systems (Turing, 1952; Segel and Jackson, 1972; Rovinski and Menzinger, 1992; Pascual, 1993; Malchow and Shigesada, 1994; Sherratt *et al.*, 1995), it has to,be studied in more detail. The following questions seem to be of primary interest. First is how the speed of the moving interface depends on the problem parameters; particularly, does the interface propagation always lead to the growth of the domain occupied by the chaotic pattern? And second, what are the limits of the system stability with respect to the excitation of chaotic oscillations and is the chaotic pattern persistent? Below we give an extensive consideration of these issues, thus providing a better understanding of the phenomenon.

In order to carry out a detailed investigation, we choose another form of the species initial distribution,

$$\begin{aligned} &u(x, 0) = u_*, \\ &v(x, 0) = v_* + A \sin\left[\frac{2\pi(x - x_0)}{S}\right] \quad \text{for } x_0 \leqslant x \leqslant x_0 + S, \end{aligned} \tag{13}$$

and

$$v(x, 0) = v_* \qquad \text{for} \quad x \leqslant x_0 \quad \text{or} \quad x \geqslant x_0 + S, \tag{14}$$

where x_0, A, and S are parameters. An advantage of the initial conditions (13) and (14) compared with (9) and (10) or (11) and (12) is that the perturbation of the species homogeneous spatial distribution is now localized and can be virtually described by two parameters: the amplitude A and the magnitude S.

The results of our computer simulations show that for this new form of the species initial distribution the

dynamics of the system stays principally the same with only slight modifications. For not too small values of A and S (see Section 5 for details), the evolution of the initial conditions leads to the formation of chaotic patterns, first inside a sub-domain, determined by the position of the initial perturbation, and then, after propagation of the interface, inside the whole domain. In case of initial conditions (13) and (14), the moving front separates a region occupied by a chaotic pattern from a region with a spatially homogeneous distribution. In order to illustrate the situation, Fig. 5 shows the spatial distribution of species u and v calculated at time $t = 1600$ for $k = 2.0$, $r = 0.4$, $H = 0.3$, $A = 0.02$, $S = 100$, and $x_0 = 1500$.

To complete this section, we want to mention that the found results do not strongly depend on the chosen

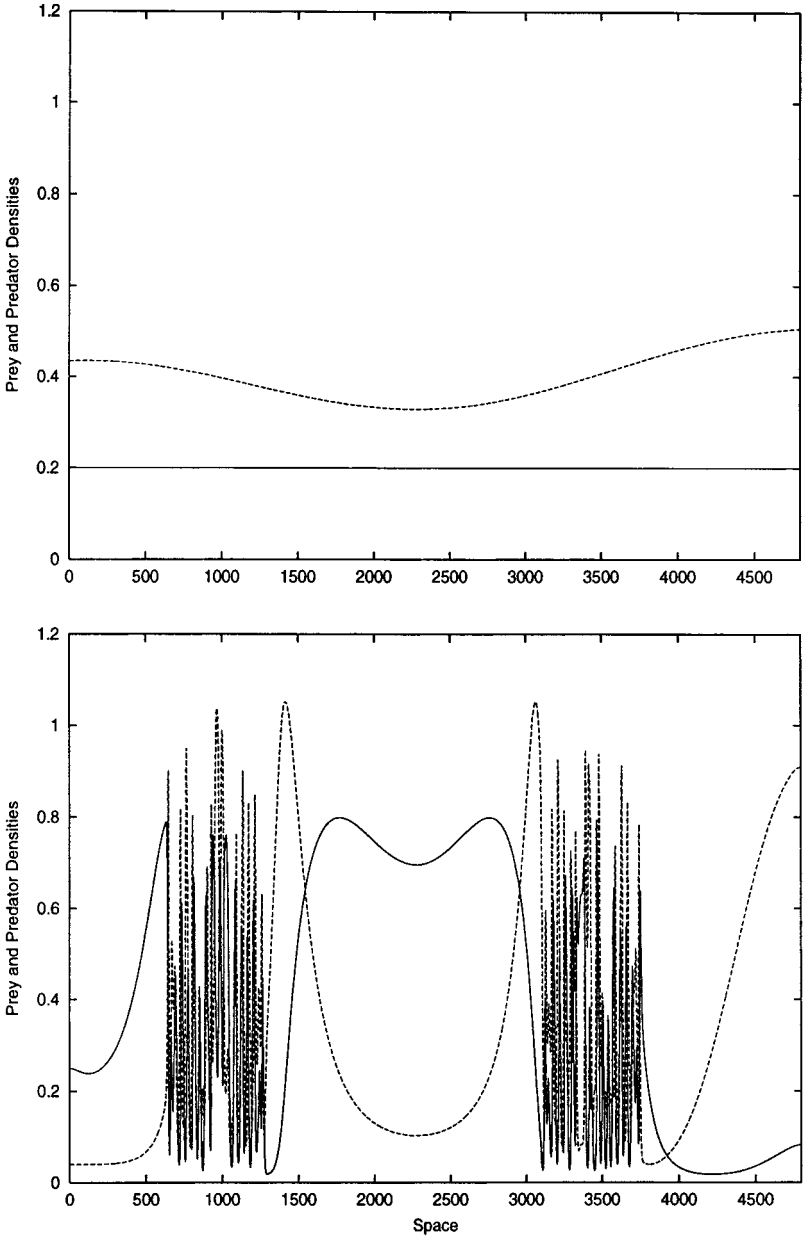

FIG. 4. Slightly inhomogeneous non-monotonic initial conditions (11) and (12) (top, for parameters $\varepsilon_1 = 0.07$, $\varepsilon = 1.5 \times 10^{-5}$, $\delta = -3.6 \times 10^{-2}$, and $L = 4800$) lead to the formation of an intermittent spatial structure (bottom, at $t = 800$). Solid line for prey, dashed for predator. Other parameters are the same as those in Fig. 2.

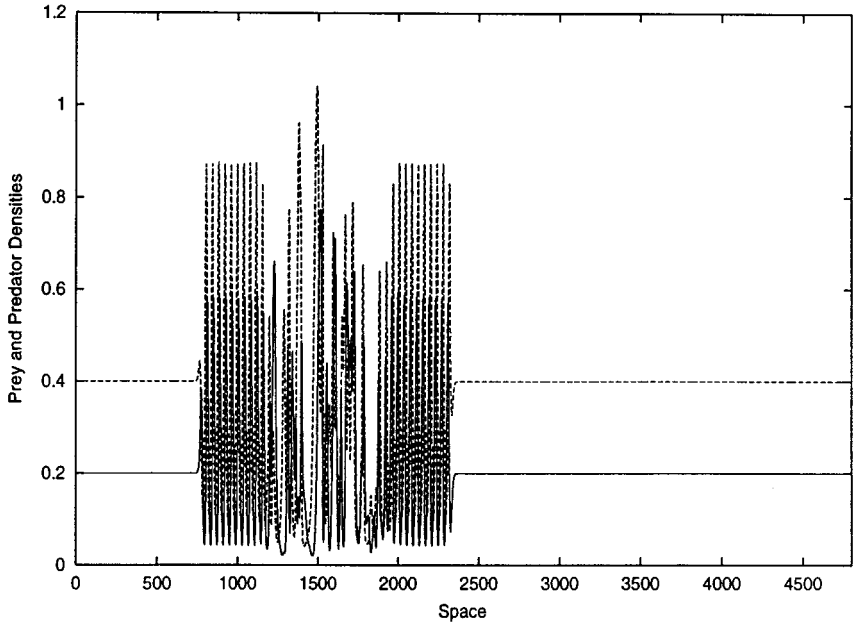

FIG. 5. Spatial distribution of species (soli line for prey, dashed for predator) calculated for $t = 1600$ for the locally disturbed homogeneous initial distribution (13)–(14) for $A = 0.02$, $S = 100$, and $x_0 = 1500$; other parameters are as in Fig. 2.

apparent asymmetry of the initial conditions considered above, where $u(x, 0)$ is constant and $v(x, 0)$ is perturbed. Other forms of initial conditions, e.g., when $u(x, 0)$ is perturbed and $v(x, 0)$ is constant or the distribution of both species is perturbed, lead to qualitatively the same dynamics of the system.

4. CALCULATION OF THE SPEED OF THE INTERFACE PROPAGATION

We begin with the calculation of the speed of the moving front (interface) by numerical simulations. Generally, a sub-domain occupied by the chaotic pattern is separated from the regular pattern by two interfaces, one of them propagating to the right and the other one propagating to the left (cf. Fig. 2, middle and bottom). Since Eqs. (5) and (6) are invariant with respect to the change $x \to -x$, we have no reason to expect that the value of the speed is different for the two interfaces. Thus, it is sufficient to consider the propagation of only one of them; the analysis presented below investigates the interface propagating to the right.

To calculate the speed, first, the dependence of the front position on time has to be calculated. The determination of the front position inevitably involves a certain convention. Here we define the front position for a given time t as a position x_{fr} where the difference between u_*, corresponding to the homogeneous stationary state in front of the interface, cf. Fig. 5, and the actual value $u(x, t)$ for the first time reaches a preassigned value δu, i.e., $|u(x_{fr}, t) - u_*| = \delta u$. Naturally, the position of the front defined in this way depends on δu. This uncertainty is not important because we are more interested in the speed of the front than in its position. One can expect that, for sufficiently small δu, the calculated value of the speed does not depend on δu.

Figure 6 (top) displays the dependence of the interface position x_{fr} on t obtained in numerical simulations for the parameter values $k = 2.0$, $r = 0.3$, $H = 0.4$ (when (u_*, v_*) is an unstable focus) and $\delta u = 0.0001$; the initial distribution of species is described by Eqs. (13) and (14). One can see that the moving front is clearly non-stationary (oscillating) and also its speed, if defined by the usual expression $dx_{fr}(t)/dt$, essentially depends on time. However, it seems more reasonable to define the speed w of the interface as the slope of the envelope; cf. Shigesada *et al.* (1986) for a similar approach. Since the envelope is apparently a straight line (except for early stages of the process, $t \leqslant 100$ in this case), this approach leads to a constant value of the speed. For the parameters of Fig. 6 (top) it is $w_{num} = 0.39 \pm 0.02$. We want to

mention that the value of the speed determined by this approach is robust to variations of δu in the interval $0 \leqslant \delta u \leqslant 0.01$.

The oscillating advance of the interface depends on the type of the stationary point (u_*, v_*). Figure 6 (bottom) shows the position of the front vs time calculated for parameters $k = 0.2$, $r = 0.6$ and $H = 0.05$ when (u_*, v_*) is an unstable node. In this case, the interface propagates as a stationary travelling wave (if being defined for not too large values of δu) and the value of the speed is given by the slope of the plot of $x_{fr}(t)$. For the parameters of Fig. 6 (bottom), we obtain $w_{num} = 1.21 \pm 0.05$.

Now we proceed to the analytical calculation of the speed of the interface. Let us mention that, in case of initial conditions (13) and (14), the chaotic spatiotemporal oscillations invade the region with a

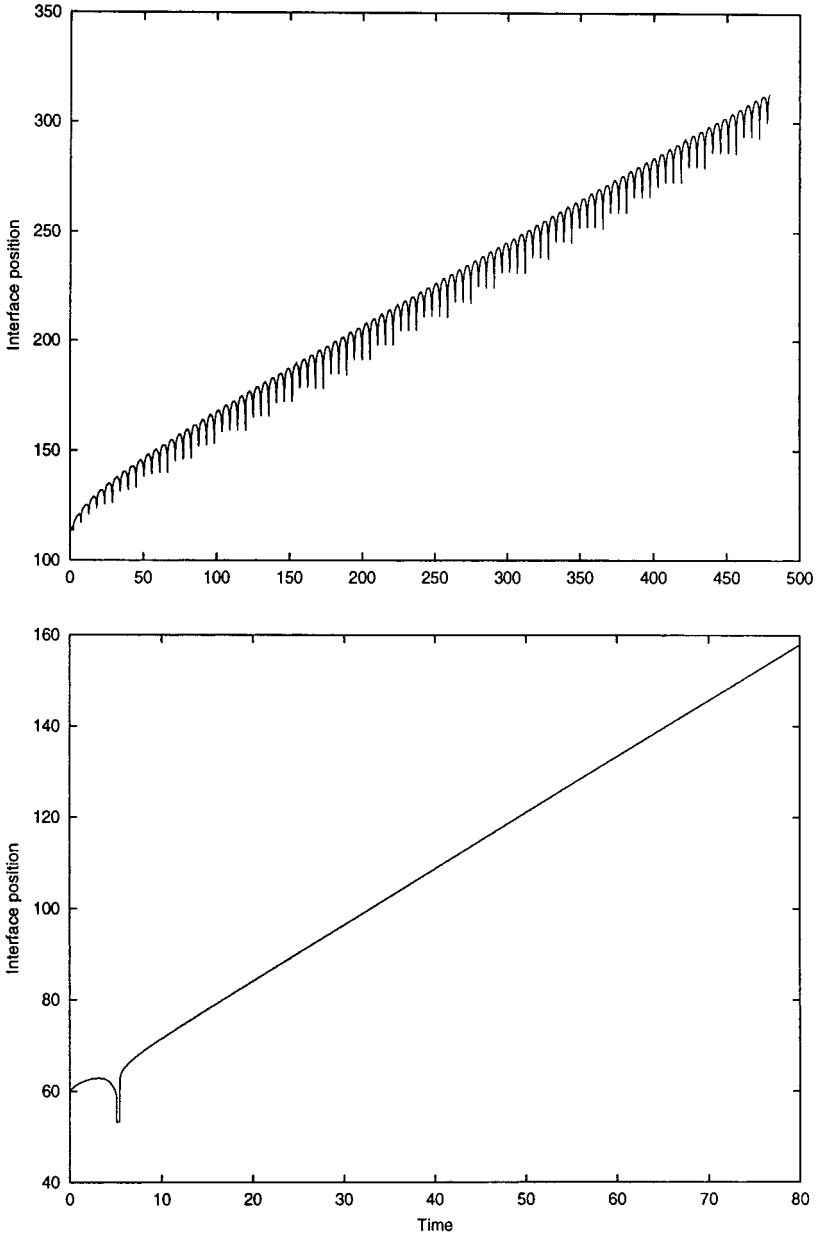

FIG. 6. The position of the interface between regular and chaotic patterns vs time for the cases of (u_*, v_*) being an unstable focus (top, for $k = 2.0$, $r = 0.3$, $H = 0.4$) and unstable node (bottom, for $k = 0.2$, $r = 0.6$, $H = 0.05$). In the first case, the speed is given by the slope of the envelope.

stationary homogeneous distribution of species. Thus, far in front of the interface, the solution of the problem (5)–(6), (13)–(14) can be written in the form of a small perturbation of the homogeneous stationary state, i.e.,

$$u(x, t) = u_* + P(x, t), \quad v(x, t) = v_* + Q(x, t), \tag{15}$$

where P, $Q \to 0$ for $x \to +\infty$.

Substituting (15) into (5) and (6) and taking into account $f(u_*, v_*) = g(u_*, v_*) = 0$, one obtains in linear approximation the following equations for P and Q,

$$P_t = P_{xx} + a_{11}P + a_{12}Q, \quad Q_t = Q_{xx} + a_{21}P + a_{22}Q, \tag{16}$$

where

$$a_{11} = \frac{\partial \tilde{f}(u_*, v_*)}{\partial u}, \qquad a_{12} = \frac{\partial \tilde{f}(u_*, v_*)}{\partial v},$$
$$a_{21} = \frac{\partial \tilde{g}(u_*, v_*)}{\partial u}, \qquad a_{22} = \frac{\partial \tilde{g}(u_*, v_*)}{\partial v}, \tag{17}$$

where $\tilde{f}$ and $\tilde{g}$ stand for the non-linear terms in Eqs. (5) and (6).

Equations (16) are linear; a standard approach for constructing a solution of a linear partial differential equation is to assume that variables x and t can be "separated;" i.e., functions P and Q can be written in the form

$$P(x, t) = p(t)\,\phi_1(x), \quad Q(x, t) = q(t)\,\phi_2(x), \tag{18}$$

where functions p, q, ϕ_1, and ϕ_2 are to be determined. Here, $\phi_1(x)$ and $\phi_2(x)$ tend to zero with increasing distance from the interface. Evidently, they must be of the same order. Thus, for simplicity, we assume that $\phi_1(x) = \phi_2(x) = \phi(x)$. Then, substituting (18) into (16), we obtain after standard transformations (e.g., Crank, 1975)

$$\frac{dp}{dt} = (a_{11} + \Pi)\,p + a_{12}q, \qquad \frac{dq}{dt} = a_{21}p + (a_{22} + \Pi)\,q \tag{19}$$

and

$$\frac{d^2\phi}{dx^2} = \Pi\phi, \tag{20}$$

where Π is a certain constant. Note that, since $\phi(x)$ must tend to zero for $x \to +\infty$, Eq. (20) has only trivial solution for $\Pi \leqslant 0$. Thus, the constant Π is positive. Denoting for convenience $\Pi = \beta^2$, we obtain from Eq. (20) that $\phi(x) = \exp(-\beta x)$.

Therefore, far in front of the advancing interface, the perturbation of the stationary homogeneous species distribution has the form

$$u(x, t) - u_* = p(t)\exp(-\beta x),$$
$$v(x, t) - v_* = q(t)\exp(-\beta x), \tag{21}$$

where $p(t)$ and $q(t)$ are the solution of system (19).

The general solution of the linear system (19) is

$$p(t) = B_1\exp(\lambda_1 t) + B_2\exp(\lambda_2 t),$$
$$q(t) = C_1\exp(\lambda_1 t) + C_2\exp(\lambda_2 t), \tag{22}$$

where B_1, B_2, C_1, and C_2 are constant and the eigenvalues $\lambda_{1,2}$ are the solutions of the equation

$$(a_{11} + \beta^2 - \lambda)(a_{22} + \beta^2 - \lambda) - a_{12}a_{21} = 0, \tag{23}$$

i.e.,

$$\lambda_{1,2} = [\beta^2 + (T/2)] \pm \tfrac{1}{2}\Delta^{1/2}, \tag{24}$$

with $T = a_{11} + a_{22}$, $\delta = a_{11}a_{22} - a_{12}a_{21}$, and $\Delta = T^2 - 4\delta$.

Now, the cases of (u_*, v_*) being (i) an unstable focus and (ii) an unstable node will be treated separately. For the first case $\Delta < 0$, and by considering Eqs. (21) and (22), it is not readily seen that the speed of the front is determined by the real part of the eigenvalues. Since $\mathrm{Re}\,\lambda = \beta^2 + (T/2)$, Eq. (21) take the form

$$u(x, t) - u_* = \tilde{p}(t)\exp\left[-\beta\left(x - \left[\beta + \frac{T}{2\beta}\right]t\right)\right], \tag{25}$$

$$v(x, t) - v_* = \tilde{q}(t)\exp\left[-\beta\left(x - \left[\beta + \frac{T}{2\beta}\right]t\right)\right], \tag{26}$$

where $\tilde{p}(t)$ and $\tilde{q}(t)$ are periodical functions. Considering the structure of Eqs. (25)–(26), we arrive at the following equation for the speed of the front:

$$w = \beta + \frac{T}{2\beta}. \tag{27}$$

The structure of Eqs. (25)–(26) is in good qualitative agreement with the numerical results, cf. Fig. 6 (top): the periodical functions $\tilde{p}(t)$ and $\tilde{q}(t)$ correspond to oscillations at the edge of the front while the other factors describe the average advance of the interface.

Thus, the spectrum of possible values of the speed depends on the unknown parameter β. However, the spectrum (27) has a lower bound, corresponding to the value $\beta_0 = (T/2)^{1/2}$. The expression for the lower bound is

$$w_{\min} = (2T)^{1/2}. \tag{28}$$

In the second case, when the stationary point (u_*, v_*) is an unstable node, $\Delta > 0$, both eigenvalues are real and the perturbation of the homogeneous stationary solution takes the form

$$u(x, t) - u_* = \exp\left[-\beta \left(x - \frac{\lambda_1}{\beta} t \right) \right] \times (B_1 + B_2 \exp[(\lambda_2 - \lambda_1) t]), \tag{29}$$

$$v(x, t) - v_* = \exp\left[-\beta \left(x - \frac{\lambda_1}{\beta} t \right) \right] \times (C_1 + C_2 \exp[(\lambda_2 - \lambda_1) t]), \tag{30}$$

where

$$\lambda_1 = \beta^2 + (1/2)(T + \Delta^{1/2}) \quad \text{and} \quad \lambda_2 = \beta^2 + (1/2)(T - \Delta^{1/2}). \tag{31}$$

Since $\lambda_2 < \lambda_1$, the term containing $\exp[(\lambda_2 - \lambda_1) t]$ vanishes for large t. Thus, in this case the solution of Eqs. (5)–(6) behaves as a stationary wave at the edge of the moving interface travelling with the speed

$$w = \beta + \frac{1}{2\beta} (T + \Delta^{1/2}). \tag{32}$$

This conclusion is in agreement with the numerical results; cf. Fig. 6 (bottom): no oscillations emerge at the edge.

The lower bound of the spectrum (32) is

$$w_{\min} = [2(T + \Delta^{1/2})]^{1/2}. \tag{33}$$

The expressions (28) and (33) provide a useful estimate of the actual value of the speed of the interface. Note that Eqs. (28) and (33) have been found analytically without any additional assumptions. To obtain these expressions, we have not referred to the particular form of parametrization, i.e., to the non-linear terms on the right-hand side of Eqs. (5)–(6). Thus, these expressions have a more general meaning and can be used also for a different choice of the functions $P(u)$ and $E(u, v)$.

Principally, Eqs. (28) and (33) give only the lower bound for the speed of the moving interface and not the exact value. In many cases (cf. Dunbar, 1986; Murray, 1989; Shigesada and Kawasaki, 1997), the actual speed of a moving front in a reaction-diffusion system coincides with the minimal possible value. However, to the best of our knowledge, this fact has not been proved rigorously for a more or less general situation. Moreover, some recent results (Hosono, 1998) indicate that this rule may be not as strict as it is sometimes considered to be. To verify this hypothesis in our case, we compare the value calculated according to (28) or (33), depending on the type of (u_*, v_*), with the value of the speed obtained in numerical simulations. For the parameters of Fig. 6, top and bottom, we obtain $w_{\min} = 0.39$ and $w_{\min} = 1.19$, respectively. Thus, the theoretical prediction is in very good quantitative agreement with the results of computer experiments and one can expect that the expressions (28) and (33) provide, at least, a good estimate for the real value of the speed of the interface propagation for other value of parameters.

In conclusion for this section, it should be mentioned that the minimal value of the speed, cf. Eqs. (28) and (33), is essentially positive. That confirms our numerical result that the chaotic pattern, once it has appeared, always invades the whole domain.

5. HIERARCHY OF REGIMES

In the previous sections, we showed that for various initial conditions the dynamics of the system (5)–(6) leads either to the formation of a regular spatio-temporal pattern or, via propagation of the "wave of chaos," to the formation of a chaotic pattern. In this section, we provide a more detailed analysis of the conditions for the formation of the two different patterns and consider their persistence.

To address the first of these issues, we calculate the "excitation diagram." The type of system dynamics with initial condition (13)–(14) is checked for a wide range of parameters A and S. We have found that the parameter plane (S, A) consists of three regions; see Fig. 7 (obtained for $k = 2.0$, $r = 0.3$, and $H = 0.4$).

The initial perturbation of the stationary homogeneous spatial distribution does not lead to any pattern formation if at least one of the parameters is small

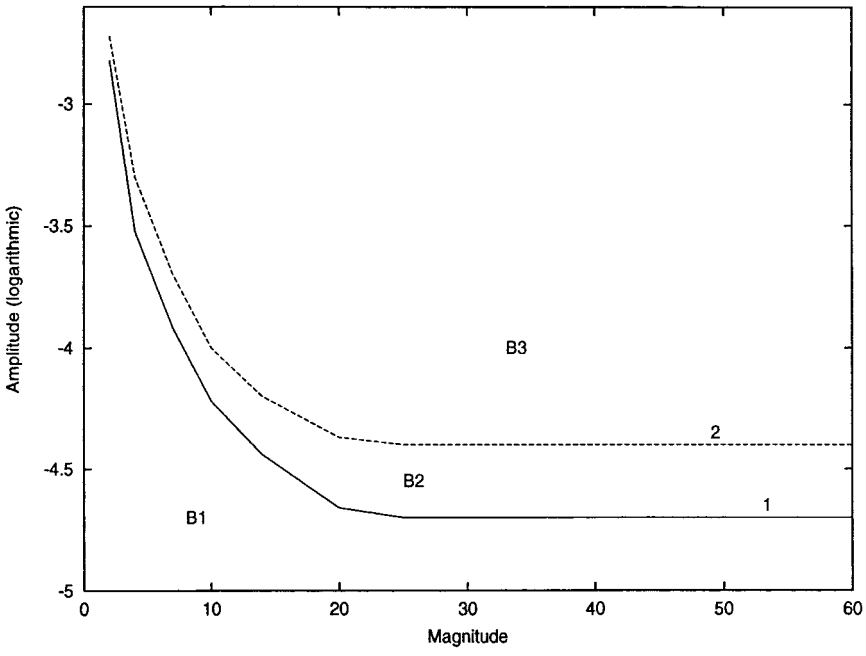

FIG. 7. A sketch of the map in the parametric (S, A) plane (semi-logarithmic) obtained for parameters $k = 2.0$, $r = 0.3$, and $H = 0.4$ for the locally disturbed initial conditions (13)–(14). Different domains correspond to the excitation of different regimes (see comments in the text).

enough (region $B1$). In this case, the homogeneous distribution is restored, the only consequence being that the values of the species densities, u and v, leave the vicinity of the steady state (u_*, v_*) and approach the limit cycle. If the values of amplitude A and magnitude S are larger (region $B2$), then the initial perturbation leads to the excitation of a regular pattern (see Fig. 2, top, as an example). Finally, for even larger values of A and S (region $B3$), the initial condition (13)–(14) leads to the excitation of a chaotic pattern according to the scenario described above. These results are also summarized in the diagram in Fig. 8; lines 1, 2, and 3 correspond to parameters from domains $B1$, $B2$, and $B3$, respectively. Note that, for the parameters of Fig. 7, the value of the

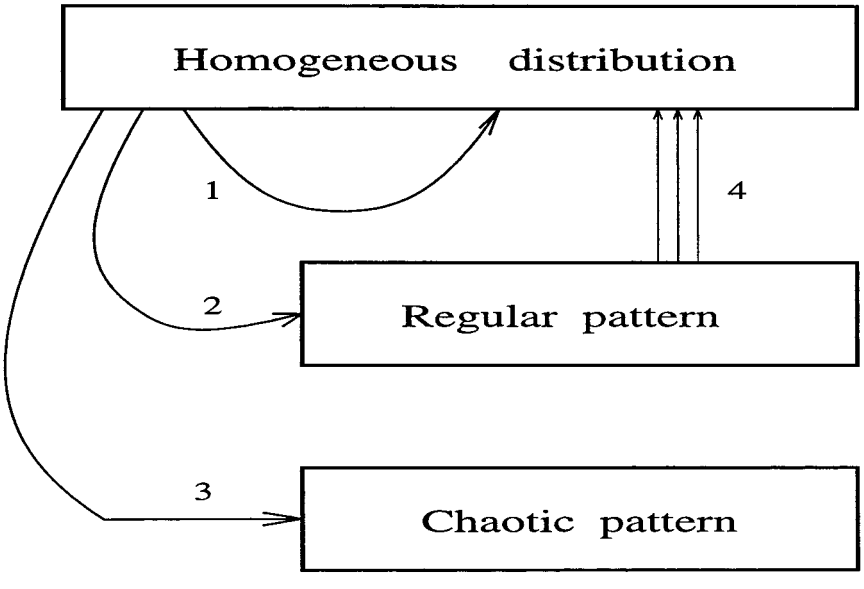

FIG. 8. Hierarchy of regimes. The arrows show allowed transitions between different regimes of the system.

stationary species concentrations, u_* and v_*, are 0.171 and 0.473, respectively, whereas a typical value of the perturbation amplitude A leading to the excitation of a chaotic pattern is quite small: 10^{-3} and less. Our numerical results show that, although particular figures can be different for a different set of parameters, the critical values of A and S remain of the same order. Thus, the limit of the system stability with respect to the excitation of chaotic oscillations is low. This fact, considered together with the results of Sections 3 and 4, leads to the conclusion that the formation of the chaotic spatio-temporal pattern is a rather typical phenomenon for a prey–predator community with oscillating local dynamics.

The next point of interest is the persistence of the patterns. To investigate this problem, we run long-term numerical simulations. Our results show that the regular pattern is not self-sustainable. This regime of the system dynamics is, in fact, the process of a very slow relaxation (with a characteristic time $\tau_{gl.rel.} \simeq 10^5$ to 10^6) to the spatially homogeneous temporally periodical solution. In this case the dynamics of the system is as follows. First, after a perturbation of the initial homogeneous state, the process of local relaxation takes place (transition 2 in Fig. 8): in each point x, the dynamical variables u and v approach the periodical solution corresponding to the limit cycle of the homogeneous system. The time scale of this process is $\tau_{loc.rel.} \simeq 10^2$ to 10^3, depending on the problem parameters. However, the periodical oscillations at different positions take place with different phases. Then, the process of the "global" relaxation begins (transition 4 in Fig. 8) which finally leads, after time $\tau_{gl.rel.} \gg \tau_{loc.rel.}$, to the synchronization of the local oscillations.

This process can also be described in terms of the spatially averaged concentrations, $\langle u \rangle$ and $\langle v \rangle$. Their temporal behaviour may be rather complicated at early stages (Petrovskii and Malchow, 1999); however, for large times, i.e., for $t \geqslant \tau_{gl.rel.}$, the trajectory in the $(\langle u \rangle, \langle v \rangle)$ plane approaches the limit cycle.

On the contrary, the chaotic pattern is persistent. In this case, there are also two different time scales. The first scale $\tau_{emb.}$ corresponds to the formation of the "embryo(s)" of the chaotic pattern; this time is estimated to be of the same order as $\tau_{loc.rel.}$. The next time scale τ_{dis} corresponds to the growth of the chaotic domain(s) and the propagation of the "wave of chaos." The value of τ_{dis} depends significantly on the problem parameters; cf. Eqs. (28) and (33). And then, after the chaotic spatio-temporal oscillations have invaded the whole region, the dynamics of the system does not undergo any principal alterations. Particularly, long-term numerical simulations (up to $t \simeq 10^6$) show that the form and size of the attractors remain unchanged in the (u, v) as well as in the $(\langle u \rangle, \langle v \rangle)$ plane.

We also want to mention that the chaotic pattern, if it appears, is stable with respect to moderate alterations of the problem parameters k, r, and H provided that the local kinetics remains oscillating. The chaotic pattern can only be suppressed by a significant increase in the value of the diffusivity, i.e., when the "diffusive length" becomes greater than the full length of the system.

6. ANALYSIS OF SPATIAL CORRELATIONS

It was stated in Section 3 that the regime of irregular spatio-temporal oscillations arising in the prey–predator model (5)–(6) can be classified as chaos. That conclusion was made based on the results of the consideration of time series of the species densities (specifically, the power spectra), see Petrovskii and Malchow (1999), and on the analysis of the sensitivity of the solutions to small perturbations (Medvinsky *et al.*, 2000). However, both approaches account for the spatial properties of the species distribution only in an implicit way. Hence, in order to provide a more quantitative insight into the phenomenon, the issue of correlativity between the temporal variations of the species at different positions in space is of significant interest.

To address this issue, we start from the standard definition of the cross-correlation function of two dynamical variables, $\psi(t)$ and $\omega(t)$,

$$K(\psi, \omega; \tau) = \lim_{T \to \infty} \frac{1}{T} \int_0^T \psi(t)\, \omega(t+\tau)\, dt \qquad (34)$$

(e.g., Nisbet and Gurney, 1982), where $\psi(t)$ and $\omega(t)$ are supposed to be centered and scaled to unit variance. Note that the translation-invariance form of Eq. (34) where K depends not separately on the moments t and $t+\tau$ but only on the time lag τ implies that the process is stationary (in the probabilistic sense).

In our case, the variables of interest are the species densities at different positions. For simplicity we set $\tau = 0$ since in this section we are more interested in spatial phenomena than in temporal behaviour. Then, formally considering the prey density at x_0 and x_1 as two different dynamical variables, we obtain from Eq. (34)

$$K(x_0, x_1) = \lim_{T\to\infty} \frac{1}{T}\cdot\frac{1}{\sigma_1\sigma_2} \times \int_0^T [u(x_0, t)-\bar{u}_0][u(x_1, t)-\bar{u}_1]\, dt, \quad (35)$$

where $\bar{u}_0, \bar{u}_1$ and σ_1, σ_2 are the mean prey density and the standard deviation, respectively, at positions x_0 and x_1.

Note that the application of Eq. (34) to the dynamics of a prey–predator system produces a number of spatial correlation functions: "prey–prey" (cf. Eq. (35)), "predator–predator" (Eq. (35) with u changed to v), and "inter-species," i.e., between the densities of prey and predator at different positions. Results of our computer simulations show that the "prey–prey" and "predator–predator" spatial correlation functions exhibit a qualitatively similar behaviour. Thus, we are going to present only the results related to "prey–prey" correlations; inter-species spatial cross-correlation will not be considered in this paper.

Strictly speaking, the function $K(x_0, x_1)$ defined by Eq. (35) does not possess translation invariance with respect to x because we consider the dynamics of the species in a bounded domain. However, the results of numerical simulations clearly show that, after the chaotic pattern has invaded the whole domain, the process becomes not only stationary but also "statistically homogeneous" in space; i.e., the dynamical properties of the system do not change from point to point. Denoting $x_1 - x_0 = \xi$, we find from Eq. (35)

$$K(\xi; x_0) = \lim_{T\to\infty} \frac{1}{T}\cdot\frac{1}{\sigma_2} \times \int_0^T [u(x_0, t)-\bar{u}][u(x_0+\xi, t)-\bar{u}]\, dt, \quad (36)$$

where $\sigma_1 = \sigma_2 = \sigma$ and $\bar{u}_0 = \bar{u}_1 = \bar{u}$. Although K formally is still a function of two variables, it does not show any dependence on x_0.

Function $K(\xi)$ calculated according to (36) is shown in Fig. 9 (for parameter values $k = 2.0$, $r = 0.4$, $H = 0.3$, $x_0 = 100$, averaging is done over the time interval from $t = 4000$ to $t = 8000$). The behaviour of $K(\xi)$ is typical for chaotic dynamics (e.g., Nayfeh and Balachandran, 1995). It should be mentioned here that the irregular oscillations with non-vanishing amplitude in $K(\xi)$ are the consequence of the finiteness of the averaging interval T; the results of our numerical simulations show that their amplitude tends to zero for increasing T. Thus, the dynamics of the system can be characterized by the correlation length, corresponding to the first zero of $K(\xi)$. For the parameters of Fig. 9, $L_{corr} \approx 30$; this value depends slightly on parameters K, r, and H. The whole domain is "split" into a number $N \simeq L/L_{corr}$ of

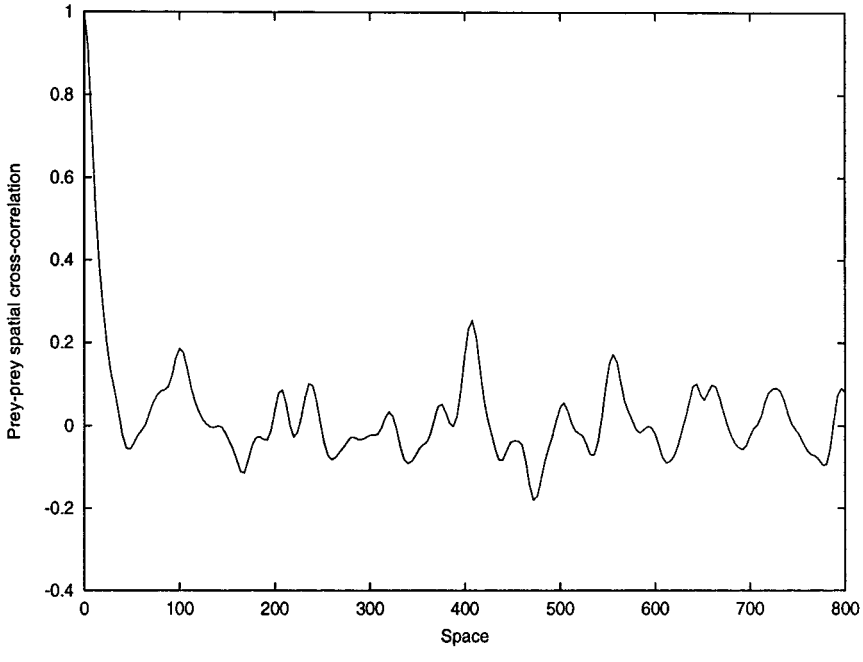

FIG. 9. Spatial cross-correlation function (36) for prey density calculated for a chaotic pattern. Parameters are $k = 2.0$, $r = 0.4$, and $H = 0.3$, and averaging is done over the time interval from $t = 4000$ to $t = 8000$.

sub-domains, their temporal behaviour being independent of each other.

Since definition (36) of the correlation function takes into account both spatial and temporal aspects, the regime of the system dynamics corresponding to the formation of a chaotic pattern can be more properly classified as spatio-temporal chaos. This conclusion is in agreement with the results of Petrovskii and Malchow (1999) where spatio-temporal chaos in a prey–predator system is described in terms of the temporal behaviour of spatially averaged species densities. We want to mention that the term "spatio-temporal chaos" used here is not just the trivial combination of the words "spatial" and "temporal" coming from the fact that the dynamics of the system (5)–(6) is spatio-temporal. The concept of chaos first appeared in connection with the temporal dynamics of spatially homogeneous time-continuous systems with at least three species. In the case of a two-species system, the dynamics of the system may become chaotic only as a result of breaking the homogeneity and the formation of spatial patterns. It seems reasonable to distinguish between these situations.

The results obtained above allow one to interpret the shape of curves 1 and 2 in Fig. 7. Actually, one can expect that the system shows different stability with respect to perturbations localized inside a single sub-domain (i.e., for $S \ll L_{corr}$) and to perturbations spread over a few domains (i.e., for $S \geqslant L_{corr}$). The change of the shape of curves 1 and 2 (from being approximately constant for large S to rapidly increasing for small S) occurs at $S \approx 25$ which is of the same order as the value of L_{corr} calculated above.

In conclusion for this section, let us mention that the standard definition (34) (or (36) for "statistical homogeneity") is hardly applicable to a regular spatio-temporal pattern because the corresponding regime of the system dynamics is transient; cf. Fig. 8. The application of Eq. (36) is formally possible for sufficiently large times $t \geqslant \tau_{gl.rel.}$ when the process becomes stationary. However, for this time the distribution of the species becomes spatially homogeneous, temporal variations of species are synchronized throughout the system, and Eq. (36) gives the obvious result $K(\xi) \equiv 1$.

7. DISCUSSION AND CONCLUSIONS

We have shown that a non-stationary irregular spatial distribution of species is a rather common phenomenon in a simple two-component prey–predator system. The formation of the pattern follows an unusual scenario. Appearing first inside one or a few "embryonic" domains, irregular spatio-temporal oscillations then invade the whole region as a result of the steady growth of the embryo(s). The dynamics corresponding to the formation of the irregular pattern exhibits spatio-temporal chaos. The interface separating a chaotic embryo from the rest of the region where the dynamics is regular moves as a travelling "wave of chaos." The results remain principally the same for a somehow different choice of functional responses $P(u)$ and $E(u, v)$, particularly, if $E(u, v)$ is given by the Ivlev formula; cf. Petrovskii and Malchow (1999).

It should be emphasized that, although this mechanism of pattern formation is in some sense more general than many of the others because it is free from usual restraints, it can hardly be regarded as a universal one, responsible for the heterogeneous spatial distribution of species in all cases. This follows particularly from the fact that the spatial correlation functions of prey and predator show a similar behaviour whereas in real communities the predator distribution is more patchy on small scale. In order to account for this phenomenon, one has to consider a model allowing for more processes than only standard diffusion, species multiplication, and grazing. A model more complicated than the one described by Eqs. (1) and (2) would early provide more mechanisms of pattern formation. Distinguishing between patterns arising because of that or another mechanism seems to be a very interesting and important problem; however, it was beyond the scope of this paper.

The results obtained in this paper show that a non-stationary irregular pattern appears as the result of the interplay between the species' spatial dispersal and their trophical prey–predator interactions. Since these two features are so typical for biological communities, it might mean that patchiness is one of the basic characteristics of the functioning of a community. The formation of patterns due to this scenario corresponds to a chaotic dynamics and thus it leads to the conclusion that spatio-temporal chaos is not a strange or exotic phenomenon but an intrinsic property of population dynamics. This seems to have significant ecological consequences; cf. Scheffer (1991). Since chaos means sensitivity to the initial condition, it means that a long-term forecast of the development of a natural population will principally never be possible. Particularly, we can calculate an average size of a single patch and the expected time of its existence but we are not able to predict when and where it will actually arise; "we can indicate the range of things that can happen, but cannot predict when they will happen" (Scheffer, 1991).

It should be mentioned that our results are consistent with some earlier studies. The "diffusion" of the species

described by Eqs. (1) and (2) is nothing but random migration of the individuals (Okubo, 1980, 1986). In this sense, our results can be considered an extension of the classical paper by Comins *et al.* (1992) where it was shown that inter-site migrations (combined with intra-site reproduction and parasitism) can give rise to complex spatio-temporal pattern formation.

Considering the results of this paper in a more general context, it should be mentioned that the phenomenon of co-existence of two different patterns (cf. Fig. 2, middle and bottom) is, of course, widely known. However, we want to stress that in all previously described cases the underlying processes are more complex and are described by much more complicated models, e.g., in terms of coupled map lattices (Kaneko, 1993).

Although we have presented a detailed study of the phenomenon, a number of open problems remain. First, the results should be generalized for systems with more spatial dimensions. As the dynamics of a system in many dimensions is usually more rich than in the 1-D case, one can expect the appearance of even more complicated phenomena. The next interesting problem is the investigation of the properties of the strange attractor responsible for the chaotic dynamics, particularly, how its dimension depends on the system parameters. And, finally, the problem as a whole should receive a more rigorous mathematical treatment. According to our results, the spatio-temporal transition between the regular and chaotic patterns is described by a system of two partial differential equations. The investigation of the conditions of existence of a solution with such an unusual behaviour is a challenging mathematical problem.

ACKNOWLEDGMENTS

We are thankful to Professors G. I. Barenblatt, W. Ebeling, and L. Schimansky–Geier for valuable discussions of the results. The helpful remarks of five anonymous referees are also appreciated.

This work was partially supported by INTAS Grant 96-2033, by NATO Linkage Grant OUTRG.LG971248, by DFG Grant 436 RUS 113/447, and by RFBR Grant 98-04-04065.

REFERENCES

Abraham, E. R. 1998. The generation of plankton patchiness by turbulent stirring, *Nature* **391**, 577–580.

Comins, H. N., Hassell, M. P., and May, R. M. 1992. the spatial dynamics of host–parasitoid systems, *J. Anim. Ecol.* **61**, 735–748.

Crank, J. 1975. "The Mathematics of Diffusion," Clarendon Press, Oxford.

Davidson, F. A. 1998. Chaotic wakes and other wave-induced behavior in a system of reaction-diffusion equations, *Int. J. Bifurcation Chaos* **8**, 1303–1313.

Denman, K. L. 1976. Covariability of chlorophyll and temperature in the sea, *Deep Sea Res.* **23**, 539–550.

Dubois, D. 1975. A model of patchiness for prey–predator plankton populations, *Ecol. Model.* **1**, 67–80.

Dunbar, S. R. 1986. Travelling waves in diffusive predator–prey equations: Periodic orbits and point-to-periodic heteroclinic orbits, *SIAM J. Appl. Math.* **46**, 1057–1078.

Ermentrout, B., Chen, X., and Chen, Z. 1997. Transition fronts and localized structures in bistable reaction-diffusion equations, *Physica D* **108**, 147–167.

Fasham, M. J. R. 1978. The statistical and mathematical analysis of plankton patchiness, *Oceanogr. Mar. Biol. Annu. Rev.* **16**, 43–79.

Flierl, G., Grünbaum, D., Levin, S., and Olson, D. 1999. From individuals to aggregations: The interplay between behavior and physics, *J. Theor. Biol.* **196**, 397–454.

Greene, C. H., Widder, E. A., Youngbluth, M. J., Tamse, A., and Johnson, G. E. 1992. The migration behavior, fine structure, and bioluminescent activity of krill sound-scattering layer, *Limnol Oceanogr.* **37**, 650–658.

Hanski, I. 1999. "Metapopulation Ecology," Oxford Univ. Press, New York.

Hanski, I., and Gilpin, M. E. (Eds.) 1997. "Metapopulation Biology," Academic Press, San Diego.

Hosono, Y. 1998. The minimal speed of travelling fronts for a diffusive Lotka–Volterra competition model, *Bull. Math. Biol.* **60**, 435–448.

Kaneko, K. (Ed.) 1993. "Theory and Applications of Coupled Map Lattices," Wiley, Chichester.

Kopell, N., and Howard, L. N. 1973. Plane wave solutions to reaction-diffusion equations, *Stud. Appl. Math.* **52**, 291–328.

Levin, S. A. 1990. Physical and biological scales and the modelling of predator–prey interactions in large marine ecosystems, *in* "Large Marine Ecosystems: Patterns, Processes and Yields" (K. Sherman, L. M. Alexander, and B. D. Gold, Eds.), AAAS, Washington.

Levin, S. A., Powell, T. M., and Steele, J. H. (Eds.) 1993. "Patch Dynamics Lecture Notes in Biomathematics," Vol. 96, Springer-Verlag, Berlin.

Mackas, D. L., and Boyd, C. M. 1979. Spectral analysis of zooplankton spatial heterogeneity, *Science* **204**, 62–64.

Malchow, H. 1996. Nonlinear plankton dynamics and pattern formation in an ecohydrodynamic model system, *J. Mar. Syst.* **7**, 193–202.

Malchow, H. 2000a. Nonequilibrium spatio-temporal patterns in models of nonlinear plankton dynamics, *Freshwater Biol.* **45**, 239–251.

Malchow, H. 2000b. Motional instabilities in predator–prey systems, *J. Theor. Biol.* **204**, 639–647.

Malchow, H., and Shigesada, N. 1994. Nonequilibrium plankton community structures in an ecohydrodynamic model system, *Nonlinear Process. Geophys.* **1**, 3–11.

Medvinsky, A. B., Tikhonov, D. A., Tikhonova, I. A., Petrovskii, S. V., and Malchow, H. 2000. Biological factors underlying regularity and chaos in aquatic ecosystems: Simple models of complex dynamics, *J. Biosc.*, to be published.

Merkin, J. H., Petrov, V., Scott, S. K., and Showalter, K. 1996. Wave-induced chemical chaos, *Phys. Rev. Lett.* **76**, 546–549.

Murray, J. D. 1989. "Mathematical Biology," Springer-Verlag, Berlin.

Nayfeh, A. H., and Balachandran, B. 1995. "Applied Nonlinear Dynamics," Wiley, New York.

Nisbet, R. M., and Gurney, W. S. C. 1982. "Modelling Fluctuating Populations," Wiley, Chichester.

Okubo, A. 1980. "Diffusion and Ecological Problems: Mathematical Models," Springer-Verlag, Berlin.

Okubo, A. 1986. Dynamical aspects of animal grouping: Swarms, schools, flocks and herds, *Adv. Biophys.* **22**, 1–94.

Pascual, M. 1993. Diffusion-induced chaos in a spatial predator–prey system, *Proc. R. Soc. London B* **251**, 1–7.

Pedley, T. J., and Kessler, J. O. 1992. Hydrodynamic phenomena in suspensions of swimming microorganisms, *Annu. Rev. Fluid Mech.* **24**, 313–358.

Petrovskii, S. V., and Malchow, H. 1999. A minimal model of pattern formation in a prey–predator system, *Math. Comput. Model.* **29**, No. 8, 49–63.

Petrovskii, S. V., and Malchow, H. 2000. Critical phenomena in plankton communities: KISS model revisited, *Nonlinear Anal.: Real World Appl.* **1**, 37–51.

Petrovskii, S. V., Vinogradov, M. E., and Malchow, H. 1999. A possible explanation of "patchiness" in a plankton community, *Trans.* (*Doklady*) *Russ. Acad. Sci.* **367**, 714–717.

Petrovskii, S. V., Vinogradov, M. E., and Morozov, A. Y. 1998. Spatial-temporal dynamics of a localized populational "burst" in a distributed prey–predator system, *Oceanology* **38**, 881–890.

Platt, T. 1972. Local phytoplankton abundance and turbulence, *Deep Sea Res.* **19**, 183–187.

Powell, T. M. 1995. Physical and biological scales of variability in lakes, estuaries and the coastal ocean, *in* "Ecological Time Series" (T. M. Powell, and, J. H. Steele, Eds.), pp. 119–138, Chapman & Hall, New York.

Powell, T. M., Richerson, P. J., Dillon, T. M., Agee, B. A., Dozier, B. J., Godden, D. A., and Myrup, L. O. 1975. Spatial scales of current speed and phytoplankton biomass fluctuations in Lake Tahoe, *Science* **189**, 1088–1090.

Rovinsky, A. B., and Menzinger, M. 1992. Chemical instability induced by a differential flow, *Phys. Rev. Lett.* **69**, 1193–1196.

Scheffer, M. 1991. Should we expect strange attractors behind plankton dynamics—And if so, should we bother?, *J. Plankton Res.* **13**, 1291–1305.

Segel, L. A., and Jackson, J. L. 1972. Dissipative structure: An explanation and an ecological example, *J. Theor. Biol.* **37**, 545–559.

Seuront, L., Schmitt, F., Lagadeuc, Y., Schertzer, D., and Lovejoy, S. 1999. Universal multifractal analysis as a tool to characterize multiscale intermittent patterns: Example of phytoplankton distribution in turbulent coastal waters, *J. Plankton Res.* **21**, 877–922.

Sherratt, J. A., Lewis, M. A., and Fowler, A. C. 1995. Ecological chaos in the wake of invasion, *Proc. Math. Acad. Sci. USA* **92**, 2524–2528.

Shigesada, N., and Kawasaki, K. 1997. "Biological Invasions: Theory and Practice," Oxford Univ. Press, Oxford.

Shigesada, J. A., Kawasaki, K., and Teramoto, E. 1986. Traveling periodic waves in heterogeneous environments, *Theor. Popul. Biol.* **30**, 143–160.

Turing, A. M. 1952. On the chemical basis of morphogenesis, *Philos. Trans. R. Soc. London B* **237**, 37–72.

Vinogradov, M. E. 1983. Open-ocean ecosystems, *in* "Marine Ecology" (O. Kine, Ed.), Vol. 5, No. 2, Wiley, New York.

Vinogradov, M. E., and Menshutkin, V. V. 1977. *in* "The Sea: Ideas and Observations on Progress in the Study of the Seas" (E. D. Goldberg, Ed.), Vol. 6, pp. –891, Wiley, Berlin.

Weber, L. H., El-Sayed, S. Z., and Hampton, I. 1986. The variance spectra of phytoplankton, krill and water temperature in the antarctic ocean south of Africa, *Deep Sea Res.* **33**, 1327–1343.

Printed in Belgium